Water Resour Manage (2012) 26:1615–1638
DOI 10.1007/s11269-012-9975-6

Runoff Estimation for an Ungauged Catchment Using Geomorphological Instantaneous Unit Hydrograph (GIUH) and Copulas

Emna Ellouze-Gargouri · Zoubeida Bargaoui

Received: 10 May 2010 / Accepted: 9 January 2012 /
Published online: 26 February 2012

Abstract A methodology is proposed to apply Geomorphological Instantaneous Unit Hydrograph to ungauged basins using Monte Carlo Simulations and copulas. The effective rainfall, input of GIUH is assumed to be unknown; it is estimated with infiltration index method (ϕ-index). Correlations are detected between this index and the characteristics of rainfall. They are modeled with copulas, and are used to derive effective rainfall hyetographs. The generated hydrographs from GIUH are analyzed and give statistically the same results: dispersion and variability for all studied characteristics (volume, peak discharge, peak time and base time). However, only these hydrographs derived from ϕ conditioned to maximum intensity distribution allow reconstituting the observed hydrographs. Moreover comparing the series of order statistics of interest output and observed series, leads to decide on the representative hydrograph of the catchment behavior.

Keywords Geomorphological instantaneous unit hydrograph · Infiltration phi-index · Copulas · Ungauged catchment

1 Introduction

van der Tak and Brass (1990) predicted a promising future for geomorphological instantaneous unit hydrograph (GIUH). Indeed, GIUH is till now still largely used as a tool of flood discharges predetermination in catchments, and particularly in ungauged ones (Kumar et al. 2002; Jain and Sinha 2003; Fleurant et al. 2006; Kumar et al. 2007; Sarangi et al. 2007). Rodriguez-Iturbe and Valdès (1979), Valdès et al. (1979), Gupta et al. (1980) and Rodriguez-Iturbe et al. (1982) linked catchment response to geomorphological characteristics and relaxed the linearity hypothesis. They introduced the velocity term in the formulation of Synthetic Unit Hydrograph (SUH).

E. Ellouze-Gargouri (✉) · Z. Bargaoui
Laboratoire de Modélisation en Hydraulique et Environnement, Ecole Nationale d'Ingénieurs de Tunis, BP 37 Ecole Nationale d'Ingénieurs de Tunis, Le Belvédère, Tunis 1002, Tunisie
e-mail: Emna.Gargouri@isetr.rnu.tn

E. Ellouze-Gargouri
Département de Génie Civil, Institut Supérieur des Etudes Technologiques de Radès, Tunis, Tunisie

Many researchers tried to develop certain aspects and approaches of the initial model. It should be noted that SUH is used when no direct observations are available. SUH can be based on models of watershed storage (Nash 1959) or based on a dimensionless unit hydrograph (Soil Conservation Service SCS 1957) or it can link hydrograph characteristics to watershed characteristics (GIUH). Gupta and Waymire (1983) showed that Strahler's classification could not be the best manner to describe the geometry of hydrographic network in hydrologic response. In fact, many other works represented the network as a function of the number of network reaches and not as a function of tributaries (Karlinger and Troutman 1985; Troutman and Karlinger 1985; Gupta and Mesa 1988). These authors expressed GIUH using the normalized width function which represents the pdf of the number of reaches for a fixed hydraulic distance from the outlet. The GIUH formulated, thus, was referred to as WFIUH (Width Function Instantaneous Hydrograph) (Franchini and O'Connell 1996). Besides, Cudennec et al. (2004) proposed the transfer function of a Gamma law based on the self-similarity of drainage characteristics. The proposed model is the pdf of the length L of the water course through the network to the outlet. Nasri et al. (2004) applied this approach to model design floods in small hillside catchments in semiarid Tunisia.

The geomorphological dispersion introduced by Rinaldo et al., (1991) is another aspect developed. These authors presented two coefficients: geomorphological dispersion coefficient which is a measure of the dispersion of a disturbance by the river network structure and hydrodynamic dispersion coefficient which is a measure of the tendency of a disturbance to disperse longitudinally as it travels downstream.

Furthermore, with the development of remote-sensing techniques, DEM models (Digital Elevation Model) and GIS (Geographical Information System), the digital representation of catchment has been possible. The integration of these techniques in GIUH allows its parameterization (Jain et al. 2000; Chandramohan et al. 2002; Sahoo et al. 2006; Kumar et al. 2007; Moussa 2008).

However, as underlined by Cudennec (2007), up to now the GIUH (Goel et al. 2000; Kumar et al. 2004; Bhadra et al. 2008), and WFIUH-type approaches remain mostly parallel, except for a few converging attempts and results.

GIUH is a very attractive model due to the parsimony of necessary inputs and the simplicity of its application. It is an effective rainfall-runoff model (Kurothe *et al.* 1997); however, it presents the disadvantage of the prior knowledge of effective rainfall (Bárdossy et al. 2006) which is particularly complicated to determine for ungauged basins. The most difficult problem is how to determine the amount of effective rainfall to route. It is a nonlinear problem that involves a variety of hydrological processes and heterogeneity of rainfall intensities, soil characteristics and antecedent conditions (Beven 2003). We find in Horton (1933), the pioneer paper, the definition of the notion of infiltration capacity. One of the models of the approximation infiltration process is the Horton process assuming that runoff is generated by rainfall intensities that are greater than the soil infiltration capacity. Index infiltration method (ϕ-index) represents the average value of infiltration capacity through the duration of effective rainfall. This method is still largely used for estimating effective rainfall and deducing flood volume for specific rainfall events. For example, the works by Kurothe *et al.* (1997) and Goel *et al.* (2000) combined the ϕ-index infiltration model with GIUH in order to derive the flood frequency distribution. The former studied an average number of 24 rainy events per each year, in Davidson catchment in the Appalachian Mountains of Western North Carolina and the latter analyzed four basins: the Davidson and three others in India, for an average number of rainy events varying from 24 to 70. These authors assumed a constant value of ϕ-index respectively, 1.125 cm/h (Davidson) and 0.015 cm/h (the three others catchments).

Similarly, Ellouze-Gargouri and Kebaili-Bargaoui (2006) used the GIUH and ϕ-index for a small catchment controlled by a headwater dam in a semi-arid zone in Central Tunisia, in order to propose a peak discharge predetermination method from rainfall data. These authors considered effective rainfall intensities as a vector of parameters of the hydrological model, and used Monte Carlo Simulation (MCS) method to generate the corresponding hydrograph components. They reconstituted peak discharges, peak times and the volumes of observed hydrographs. The exploitation of the results of all simulations allowed deducing empirical relations characterizing the basin behavior in accordance with peak discharges, peak times, base times and runoff volumes. Besides these authors underlined a log-log linear relationship between the ϕ index of rainy event and maximum rainfall intensity (I_{max}) recorded and based on 5 min for a specific event. This kind of relationship has been further generalized for other catchments in the same geographic region (Gargouri-Ellouze and Bargaoui 2009). They used multivariate approaches based on rank statistics to investigate the nonlinear dependence between the two hydrological variables: ϕ-index and I_{max}. They revealed the importance of this dependence (Kendall's tau varies from 0.47 to 0.91). The correlation was modeled with copulas, which presently find a large echo in hydrological community (De Michele and Salvadori 2003; Favre *et al.* 2004; Grimaldi *et al.* 2005; De Michele *et al.* 2005; Salvadori and De Michele 2006; Zhang and Singh 2006; Genest and Favre 2007; Bárdossy and Li 2008; Gargouri-Ellouze and Chebchoub 2008).

In the perspective of the applicability of the GIUH to ungauged basins, we suggest to (1) relax the prior knowledge of effective rainfall, since runoff volumes and hydrographs are unavailable, we have to introduce uncertainties in its amount and its temporal structure; and (2) investigate and eventually exploit the dependence between ϕ-index and rainfall characteristics in order to derive hydrograph's components.

The proposed methodology is (1) to generate hydrographs with MCS, (2) to analyze the dispersion of their characteristics (peak discharges, peak times, base times and the volumes), (3) to study if the coupling between ϕ-index and rainfall characteristics, reconstitutes the observed hydrographs and (4) to compare these methods of ϕ-index estimation and their impact on GIUH outputs.

This paper is organized as following: we begin by a brief presentation of the GIUH model and the estimation of effective rainfall with the infiltration index method (ϕ-index). Then we expose the stochastic generation of simulated hydrographs and the method of the analysis of outputs. In the third section, we present studied data. The relationship between the ϕ-index and the rainfall intensity characteristics (maximum intensity, average intensity and duration) is underlined and the modeling with copulas is exposed. The last section illustrates the obtained results for the case of a basin in Central Tunisia.

2 Methodology

The aim of this work is to enable applying the GIUH to ungauged basins, knowing that there are only catchment geomorphological data and rainfall hyetograph. The main hypothesis is the lack of knowledge of effective rainfall volume and intensities. The second hypothesis is that the runoff is Hortonian. This is considered as pertinent to explain the hydrological response of watersheds in semi-arid climates but also in the conditions of heavy rain intensity; it is generally admitted that even for natural soils, which present a high hydraulic conductivity in tempered and humid climates, there can be an infiltration capacity lower than maximum intensities of registered precipitations (Musy and Higy 2004). Thus, the effective rainfall can be deduced from the ϕ-index.

2.1 GIUH Model

Nadarajah (2007) and Bhunya et al. (2007) derived SUH for a group of probability distributions, including the log Normal, Gamma, inverse Gamma, Beta, Kumaraswamy, two- sided power, Pareto, inverse Gaussian, F, Weibull, Chi-square and the Fréchet distribution. Since GIUH is considered as a SUH (see above), it may be expressed as probability distribution (pdf of the travel times to the basin outlet of the water droplets randomly and uniformly distributed over the catchment); researchers, e.g. Jin (1992) and Bhunya et al. (2008), related GIUH's parameters (probability distribution parameters) to catchment characteristics and specifically to Horton's ratios.

We use Nash based GIUH model. The Nash cascade model *h(t)* (two parameter Gamma distribution) is given by (1), where the parameters are: *K* (2) for scale and *N* (3) for shape.

In addition, Rosso (1984) equated the product of the time to peak and peak flow of GIUH with the product of the time to peak and peak flow of the Nash model IUH, using multiple regression analysis to solve this equation. Rosso (1984) obtained the scale parameter *K*(2) and shape parameter *N* (3).

$$h(t) = \frac{\left(\frac{t}{K}\right)^{N-1} exp\left(\frac{-t}{K}\right)}{K\Gamma(N)} \tag{1}$$

$$K = 0.7\left(\frac{R_A}{R_B R_L}\right)^{0.48} L_\Omega U^{-1} \tag{2}$$

$$N = 3.29\left(\frac{R_B}{R_A}\right)^{0.78} R_L^{0.07} \tag{3}$$

With t is the time in seconds, L_Ω is the length of the highest order stream in kilometers, R_L, R_A and R_B (Eagleson 1970) are Horton's ratios respectively of the length, the area and the bifurcation of catchment. In (2), K is in seconds and the velocity U is expressed in meters per second.

We adopt the model of Nowicka and Soczynska (1989), which expresses the velocity U (4) as a function of effective rainfall intensity, duration and geomorphological indexes.

$$U = \frac{1.17(A_\Omega I_r t_r)^{2/3}\alpha_\Omega}{L^{2/3}} \tag{4}$$

$$\alpha_\Omega = \frac{{S_\Omega}^{1/2}}{n_\Omega {b_\Omega}^{2/3}} \tag{5}$$

Where A_Ω is the total area of catchment in square kilometers, I_r is the effective rainfall intensity in centimeters per hour, t_r is its duration in hours and L is the length of the main stream in kilometers. The velocity U is in meters per second. The term α_Ω is the kinematic wave parameter of the highest order stream, with S_Ω is the slope; n_Ω is the Manning roughness coefficient and b_Ω the width in meters.

The resulting hydrograph for an effective rainfall composed of a succession of constant intensities per interval is expressed as an integral of convolution:

$$Q_c(t) = A_\Omega \int_0^t h(\tau) i_r(t-\tau) d\tau \quad (6)$$

It should be noted that *U* varies from one interval of time to another. Consequently, *K* also varies.

2.2 Effective Rainfall Estimation

Assuming that the generation runoff process is Hortonian, the effective rainfall intensities are estimated from ϕ–index method (7) which remains despite its rudimentary character. It is a method still largely used (Kurothe et al. 1997; 2001; Beven 2003).

$$\begin{aligned} I_{rj} &= (I_j - \phi) \quad j = 1\ldots\ldots k \quad \phi < i_j \\ I_{rj} &= 0 \quad si \quad \phi \geq i_j \\ t_r &= k\Delta t \end{aligned} \quad (7)$$

With:

ϕ infiltration index (mm/h);
I_{rj} effective rainfall intensity at time $t_j = j\Delta t$ (mm/h)
I_j rainfall intensity at time $t_j = j\Delta t$ (mm/h)
t_r effective rainfall (h)
Δt time increment (h)
k total number of time increment.

2.3 Stochastic Generation of Simulated Hydrographs

We consider the effective rainfall intensities as a vector of model parameter. The vector components are estimated from the knowledge of ϕ-index for each event. Each rainy event is separately considered without presuming its occurrence probability. The generation process of hydrographs is as follows:

- Data insertion: geomorphological parameters and rainfall hyetograph with constant time increment for all simulations.
- Draw the different values of ϕ-index in a distribution conditioned to rainfall characteristic $F(\phi|\cdot)$, using MCS. The details of this step are given in the Section 3.
- For each ϕ-index value, the different components of effective rainfall are calculated.
- Simulation of different hydrographs for each estimated effective rainfall vector.
- Statistical analysis of simulated hydrographs.

2.4 Analysis Method of the Results of Simulations

In order to interpret statistically the simulated hydrographs for each rainy event (E_i), the characteristics of generated hydrographs (volume (*V*), peak discharge (*Qp*), peak time (*tp*) and base time (*tb*)) are classified; their percentiles (25th, 50th and 75th) are analyzed using box- plots. The interpretation of box-plots allows studying the range of simulated values and the outliers. Moreover, for selecting the design hydrographs, we constitute the series of order statistics corresponding to each output ($V_{(i)}$, $Qp_{(i)}$, $tp_{(i)}$ and $tb_{(i)}$, i corresponding to 10th percentile, 20th, 30th …), and we use Q-Q plots to compare each order statistics set to the observed one. In accordance with the interest output, the one which compares the best may represent the typical hydrograph of the catchment behavior. Our main interest output is the peak discharge and volume, consequently the typical hydrograph corresponds to peak discharge (or volume) order statistics set, which proves to come from populations with the same distribution as the observed one.

3 Data

The studied site is a small catchment: Saddine 1 (Fig. 1). It is near Makthar in Tunisia (Northern latitude 35°48’06” and Eastern longitude 9°04’09”) in a mountainous zone, monitored by the DGACTA (Direction Générale des Aménagements et Conservation des Terres Agricoles) and the IRD (Institut de Recherche et Développement) from 1992 to 2000, within the framework of the HYDROMED project (Programme de recherche sur les lacs collinaires dans les zones semi-arides du pourtour méditerranéen). This catchment is controlled by a headwater dam whose filling was realized in 1992. The dominant geological class for this basin is clays, coquinas, evaporites with a clayey sandstone alternation. The catchment is thus considered as quasi-impermeable to impermeable (Hermassi 2000). Table 1 deals with the basin geomorphological characteristics, and shows that the relief is high (R5 according to I.R.D. classification) and the slope is important (100 m/km) which help rapid runoff. The most important recorded event during the period of observation is the September 4th, 1995, with a total rainfall of 39.5 mm, a duration of 13 min, and a maximal intensity throughout 5 min reaching 324 mm/h. The maximum discharge is estimated to 85 m^3/s and runoff volume is evaluated to 67200 m^3, by reconstituting the water balance of storage. The observed ϕ-index is estimated to 162 mm/h.

We have a sample of 55 hydrological events (hyetographs and runoff volumes). However, only a sample of 20 events is complete (hydrographs and hyetographs). The latter covers a large value range of total depth rainfall (P), rainfall duration (D), rainfall maximum intensity (I_{max}), rainfall average intensity (I_{moy}), runoff volumes (V) and peak discharges (Qp) (Fig. 2, Table 2). The analysis of Fig. 2 and Table 2 shows the variation coefficients of P, D, I_{max}, I_{moy}, V and Qp respectively of: 1.0, 1.2, 0.9, 1.0, 1.1 and 1.9, which indicates a high variability for rainfall as well as hydrological basin behavior. Moreover, the confrontation of rainfall hyetograph and runoff volume series allows establishing ϕ-index set. Table 2 shows a high variability of ϕ-index from an event to the other (variation coefficient equal to 0.91), contrary to the hypothesis of Eagleson (1972), Kurothe *et al.* (1997) and Goel *et al.* (2000) who adopted a constant value by catchment.

Furthermore, for the analysis of rainfall, we take into consideration the 55 observed rainfall hyetographs (I). These hyetographs are with a reference time increment Δt equal to 5 min. We, thus, constitute the different sets of rainfall characteristics (I_{max}, I_{moy}, D and P) through the observation period. The marginal distributions of variables: I_{max}, ϕ-index, D, I_{moy} and P are fitted using (HYFRAN[1]). The parameters are estimated by the maximum-likelihood method, and the goodness-of-fit is achieved with the Chi-square test. Table 3 recapitulates the main characteristics of the variable distributions.

[1] Software developed by INRS-ETE, Chaire en hydrologie statistique (HYDRO-QUÉBEC / ALCAN / CRSNG).

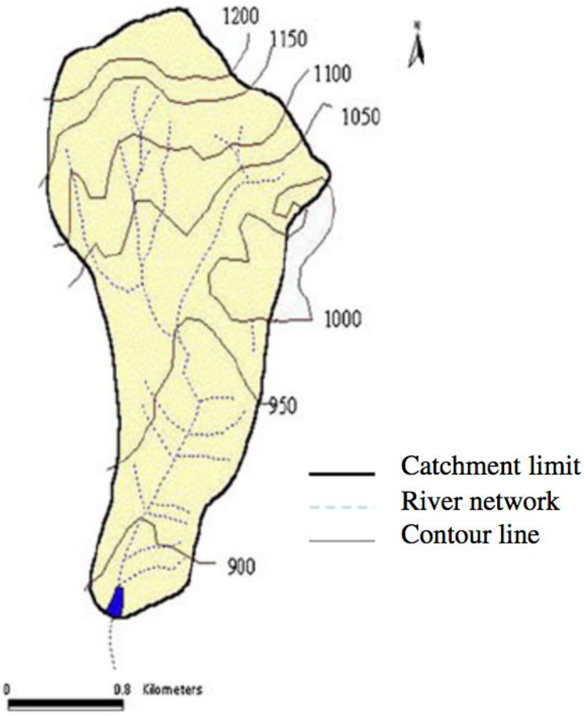

Fig. 1 Saddine 1 catchment

3.1 Investigation and Modeling the Relationship between Φ-Index and Rainfall Intensity Characteristics

The impermeable character of the catchment and the semi-arid climate allow assuming a Hortonian runoff. Consequently, the use of ϕ-index method for the estimation of effective rainfall intensities is possible. Besides assuming the works by Ellouze-Gargouri and Kebaili-Bargaoui (2006) and Gargouri-Ellouze and Bargaoui (2009) who underlined the relationship between ϕ-index and I_{max}, a supplementary investigation is achieved between ϕ-index and other rainfall characteristics such as rainfall depth (P), average intensity (I_{moy}) and rainfall duration (D). The main interests of establishing this relationship is to remove the constraint of the ϕ-index determination of the knowledge of runoff hydrographs, and therefore, estimating ϕ-index for ungauged basins. For this purpose, the first step is the identification

Table 1 Geomorphological characteristics of Saddine 1 catchment

Characteristic	Value
A_Ω	3.84 km²
Ω	3
L	3.5 km
L_Ω	1.32 km
Specific height	158 m
Relief Class	R5
Gravelus index	1.39
S_Ω	0.1 m/m
Maximum altitude	1250 m
Minimum altitude	842 m
R_L	1.62 with R^2=0.67
R_A	5.27 with R^2 =0.994
R_B	2.45 with R^2=0.85

A_Ω: Area; Ω: Catchment order; L: Stream main length; L_Ω: Stream length of highest order; S_Ω: Average slope; R_L: Length ratio; R_A: Area ratio; R_B: Bifurcation ratio

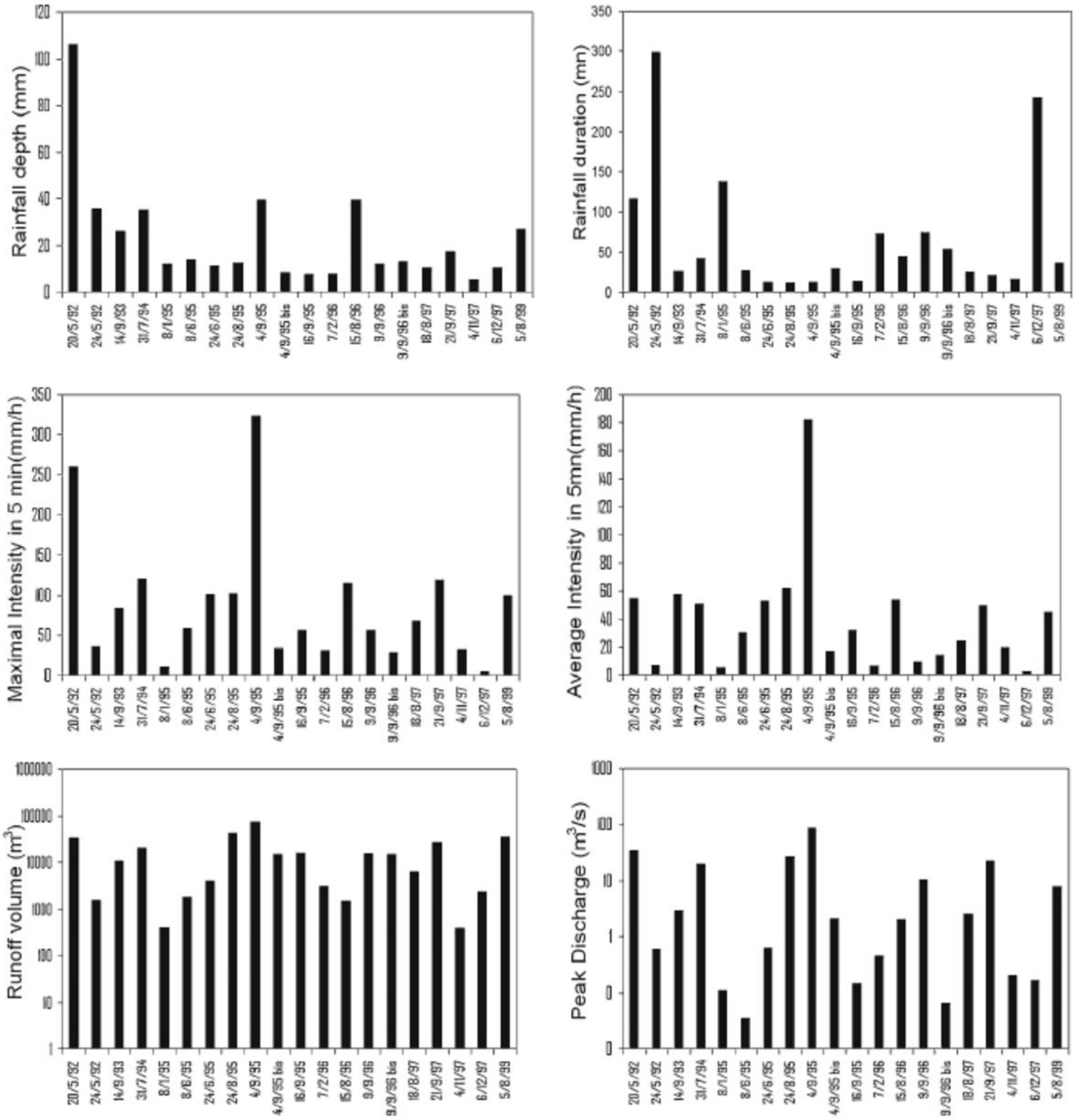

Fig. 2 Characteristics of selected hydrological events

of dependence between ϕ-index and rainfall characteristics (I_{max}, I_{moy}, D and P), then the modeling of the relationship (if it exists) with copulas, adopting the methodology used by Gargouri-Ellouze and Chebchoub (2008). Furthermore, for the validation of the modeling, we exclude four hydrological events (20/5/92, 24/5/92, 14/9/93 and 31/7/94).

3.1.1 Investigation

To measure the association between ϕ-index and rainfall characteristics, the rank correlation coefficient Kendall's tau (τ) (Joe 1997) is used for the characterization of dependence. The Kendall coefficient of rank correlation can be used for revealing dependence of two qualitative characteristics, provided that the elements of the sample can be classified with respect to these characteristics (Prokhorov 2002). This coefficient, which measures the non-linear dependence, integrates the rank of observations rather than their value. Therefore, the value itself is not so relevant than its rank among other values. To sum up, the more the Kendall's τ is higher the more the dependence is important.

Table 2 Characteristics of studied events

Event	P (mm)	D (min)	I_{max} (mm/h)	I_{moy} (mm/h)	V (m^3)	Qp (m^3/s)	tp (min)	tb (min)	ϕ (mm/h)
20/5/92	106	116	260.0	55	33059	34.70	25	60	166.0
24/5/92	36	299	36.0	7	1509	0.60	25	85	26.2
14/9/93	26	27	84.0	58	10657	3.00	60	120	58.0
31/7/94	35.5	42	120.0	51	20843	19.80	30	60	73.0
8/1/95	12	138	10.0	5	400	0.10	60	190	9.0
8/6/95	14	28	58.8	30	1768	0.04	-	-	53.0
24/6/95	11.5	13	101.0	53	3980	0.60	50	470	87.8
24/8/95	12.5	12	102.0	63	41940	26.70	20	95	5.5
4/9/95	39.5	13	324.0	182	67200	85.60	15	29	162.0
4/9/95bis*	8.5	30	33.6	17	15164	2.10	50	200	10.6
16/9/95	7.5	14	56.0	32	16055	0.10	60	-	13.1
7/2/96	8	73	31.2	7	3152	0.40	5	360	21.3
15/8/96	39.5	44	115.0	54	1476	2.00	10	-	103.2
9/9/96	12	74	56.6	10	15573	10.40	25	35	13.1
9/9/96bis*	13	53	28.8	15	15030	0.10	40	-	13.1
18/8/97	10.5	26	68.4	24	6338	2.60	45	225	48.4
21/9/97	17.5	21	118.8	50	26393	22.30	25	85	38.8
4/11/97	5.5	16	32.4	20	383	0.20	95	240	31.2
6/12/97	10.5	243	4.8	3	2336	0.20	135	335	3.8
5/8/99	27	36	99.6	45	35093	7.90	60	390	47.3

P: rainfall depth; *D*: rainfall duration; *Imax*: rainfall maximum intensity; *Imoy*: rainfall average intensity; *V*: runoff volume; *Qp*: peak discharge; *tp*: peak time; *tb*: base time; ϕ: infiltration index. 4/9/95 event occurred at 16 h50 and 4/9/95 bis*occurred at 23 h45. 9/9/96 occurred at 5 h15 and 9/9/96 occurred at 14 h55

A test of independence can be adopted for Kendall's τ, since under the null-hypothesis H_0, this statistic is close to Normal distribution with zero mean and variance $2(2n+5)/[9n(n-1)]$ (n size of sample). As a result H_0 would be rejected at an approximate level α if $|\tau| > z_{\frac{\alpha}{2}}\sqrt{[2(2n+5)]/[9n(n-1)]}$. For α=5%, $z_{\alpha/2}$ =1.96. Let z^* represent the quantity $z_{\frac{\alpha}{2}}\sqrt{[2(2n+5)]/[9n(n-1)]}$.

Table 4 deals with τ's values and their corresponding statistics for the different couples (ϕ, I_{max}), (ϕ, I_{moy}), (ϕ, D) and (ϕ, P). The analysis of Table 4 shows that H_0 independence hypothesis is rejected for the first three couples and accepted in the latter. Consequently, ϕ depends on I_{max}, which confirms the previous works; in addition, ϕ depends on I_{moy}, which implicitly depends on event duration. Indeed, the correlation between ϕ and D gives a τ's value equal to -0.41 (z*=4.20) i.e. the more the duration increases the more ϕ decreases. As

Table 3 Variable distribution and their characteristics

Variable X	Distribution	Mean μ	Standard deviation σ	Parameter position X_0	p-value
I_{max} (mm/h)	Exponential	46.5	42.6	3.9	0.94
ϕ-index (mm/h)	Exponential	32.4	29.2	3.2	0.33
D (min)	Exponential	77.9	67.3	10.6	0.09
I_{moy} (mm/h)	Lognormal	2.6	0.97	-	0.33
P (mm)	Exponential	13.3	9.00	4.3	0.19

Table 4 Kendall's τ values and their z* statistics

Couple	Sample size	τ	z^*	H_0
(ϕ, I_{max})	51	0.72	0.19	rejection
(ϕ, I_{moy})	51	0.57	0.19	rejection
(ϕ, D)	51	-0.42	0.19	rejection
(ϕ, P)	51	0.18	0.19	acceptation

I_{max}: Maximum rainfall intensity; I_{moy}: Average rainfall intensity; D: rainfall duration; P: rainfall depth τ: Kendall's tau; z^*: test statistic; H_0: null hypothesis

a conclusion the maximum intensity plays the most significant role, followed by average intensity and finally by duration, but the rainfall depth seems to have no importance. Therefore, in this paper, we only focus and exploit the following relationships: (ϕ, I_{max}) (ϕ, I_{moy}) and (ϕ, D).

3.1.2 Modeling with Copulas

We adopt the copulas for the modeling of the joint cumulative distribution function of pairs (I_{max},ϕ), (ϕ, I_{moy}) and (ϕ, D). Indeed, the fundamental idea is that we can model the dependence between ϕ - I_{max}, ϕ - I_{moy} and ϕ - D independently from the marginal distributions.

Among parametric copulas, we select Archimedean copulas with one parameter (a) which directly depends on Kendall'τ (Schweizer and Sklar 1983). They are easily constructed and have been largely used in hydrology (De Michele and Salvadori 2003; Favre et al. 2004; Grimaldi et al. 2005; De Michele et al. 2005; Bárdossy 2006; Salvadori and De Michele 2006; Zhang and Singh 2006; Bárdossy and Li 2008). They are completely defined by a generator (φ) (Genest and Mackay 1986). For the goodness-of-fit of copulas, the methodology of Gargouri-Ellouze and Chebchoub (2008) is adopted: we select among three models (Gumbel, Frank and Clayton, see Appendix 1 for details) by comparing the empirical versions of the functions K, J, M, L and R (Venter 2002, 2003, see Appendix 2 for details) and the theoretical versions and also by using bivariate χ^2 test as proposed by Hürlimann (2004) (see Appendix 3 for details). Consequently, for each couple, one copula is estimated according to Kendall's τ.

Based on this methodology, Gumbel copula is adopted for (ϕ, I_{max}) and (ϕ, I_{moy}) with a parameter a respectively of a_{Imax}=4.8 and a_{Imoy}=3 and Frank copula is adopted for (ϕ, D) with a parameter a_D=-4.4. Thus, we can generate ϕ-index conditioned to I_{max}, I_{moy} and D. The main idea of copulas is to deal with the couple $(F_X(X), F_\phi(\phi))$ and not with the couple (X, ϕ). One uses the random vector $(U = F_X(X), V = F_\phi(\phi))$ which has uniform marginals on [0, 1]. Therefore, in order to simulate the couples (U, V) one has to use the conditional distribution of V knowing U.

Figure 3a to c, show the simulated and observed values for each studied couples. We note that the observed values are reconstituted for the pairs ϕ-index conditioned to I_{max} and I_{moy}, even those used for the validation. However, it is not the case for ϕ-index conditioned to D (Fig. 3c), several values are not reconstituted. This may be due to the weakness of the relationship between ϕ-index and D (τ=-0.42) and the choice of the copula model. Other types of copulas which model negative correlations should be tested. Therefore, we suggest prospecting only the couples (I_{max}, ϕ) and (I_{moy}, ϕ). It is worth noting that during the simulation of couples (ϕ, I_{max}) ϕ is rejected when ϕ is greater than I_{max} (unfeasible case).

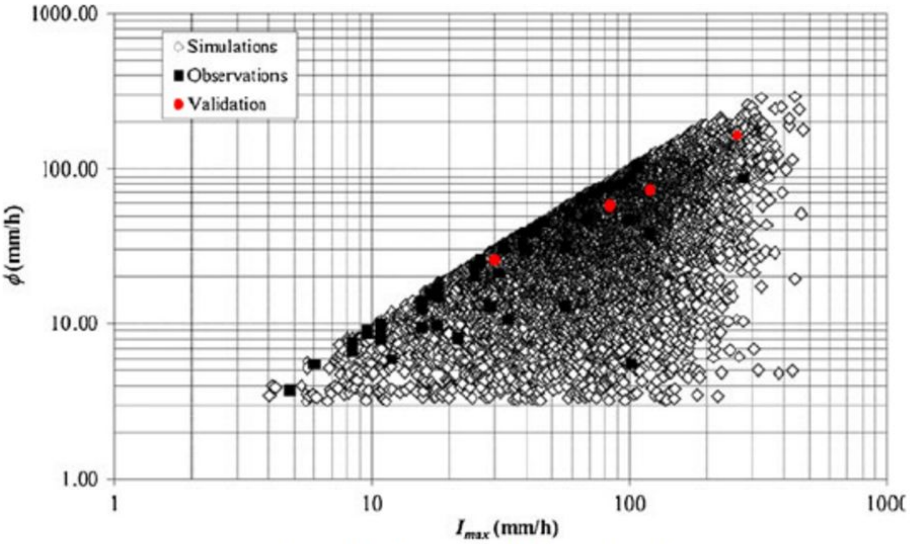

(a) ϕ-index conditioned to I_{max}

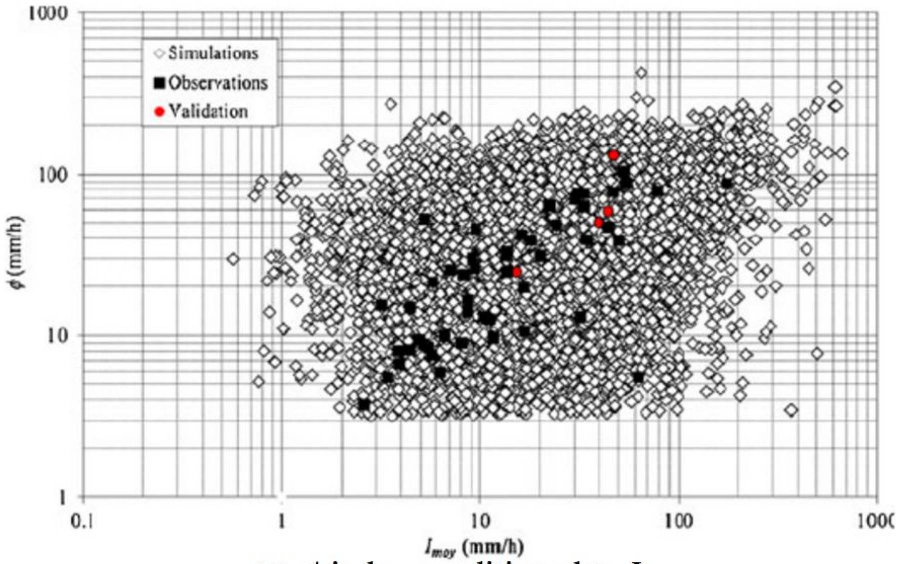

(b) ϕ-index conditioned to I_{moy}

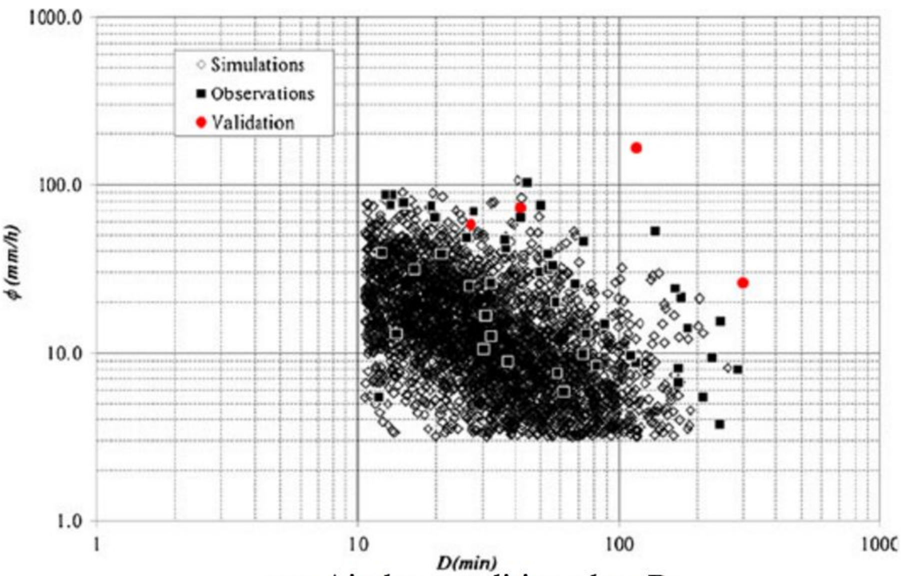

(c) ϕ-index conditioned to D

Fig. 3 **a** ϕ-index conditioned to *Imax*. **b** ϕ-index conditioned to *Imoy*. **c** ϕ-index conditioned to *D*

In order to understand and exploit these correlations, we represent in Fig. 4a and b the isolines of simulated couples (I_{max}, ϕ) and (I_{moy}, ϕ). These isolines correspond to *Intensity- ϕ−index- Frequency* curves. They give for each fixed intensity (maximum

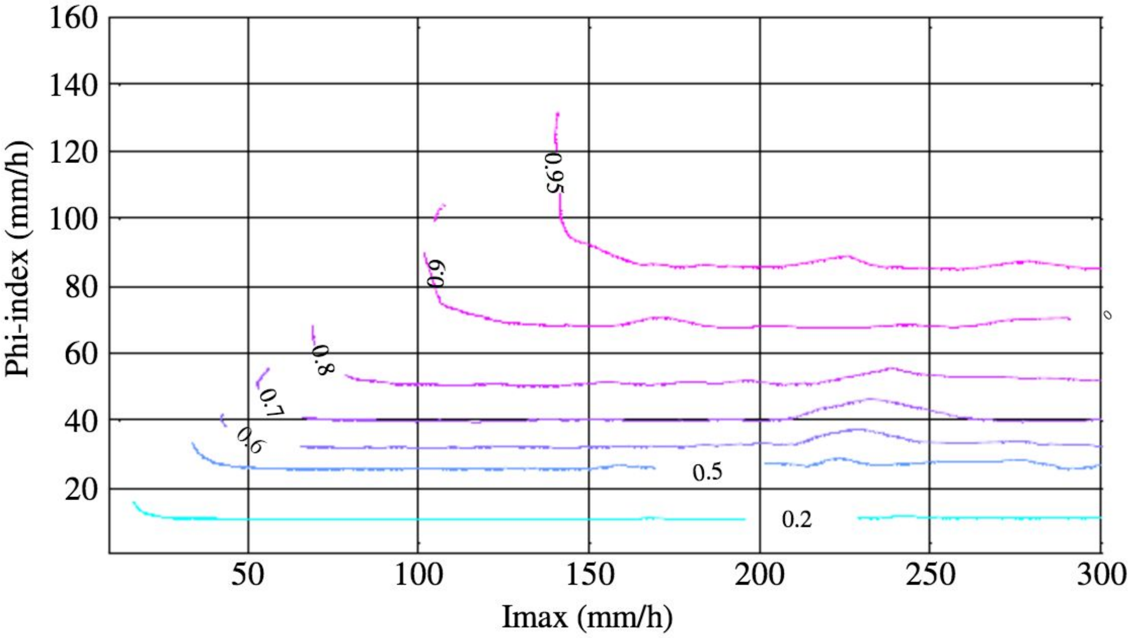

(a) Maximum Intensity - ϕ -index – Frequency

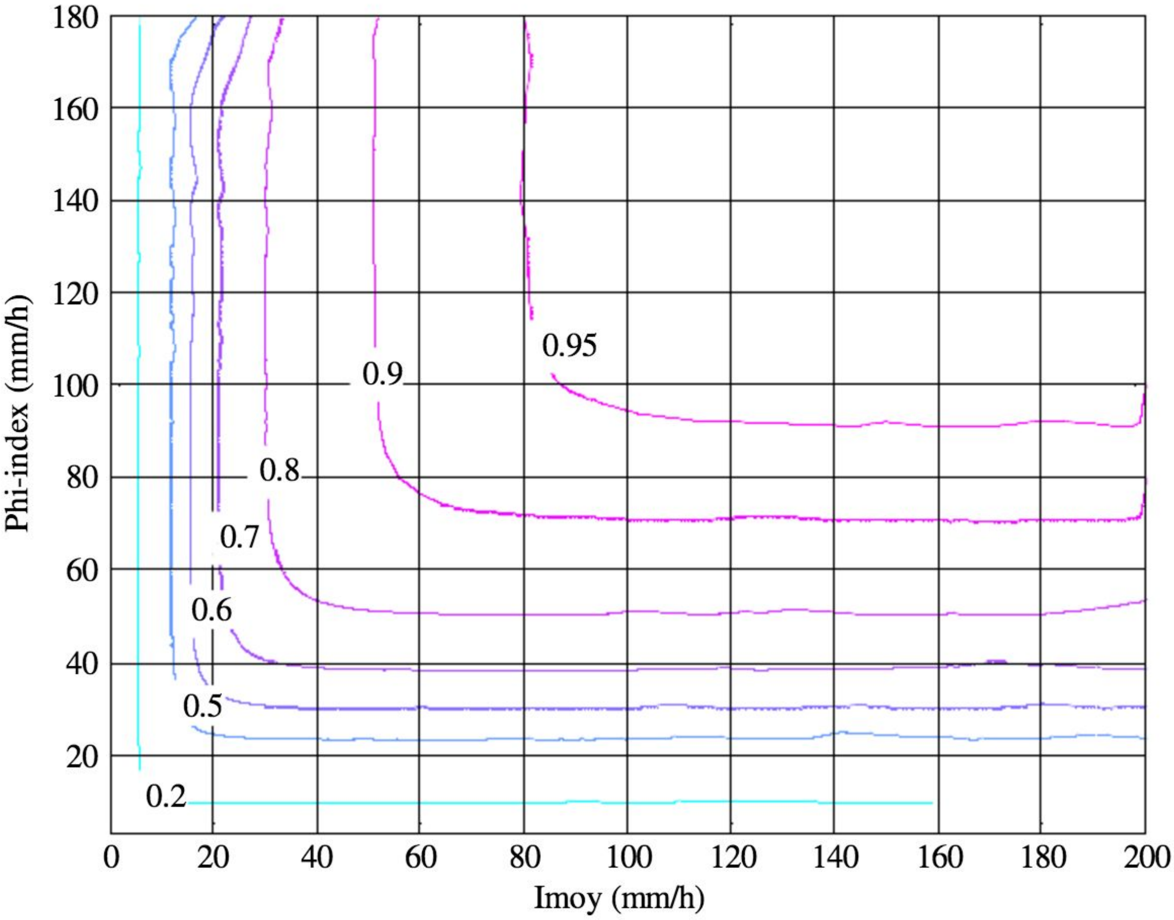

(b) Average Intensity - ϕ -index – Frequency

Fig. 4 **a** Maximum Intensity -ϕ-index – Frequency. **b** Average Intensity -ϕ-index – Frequency

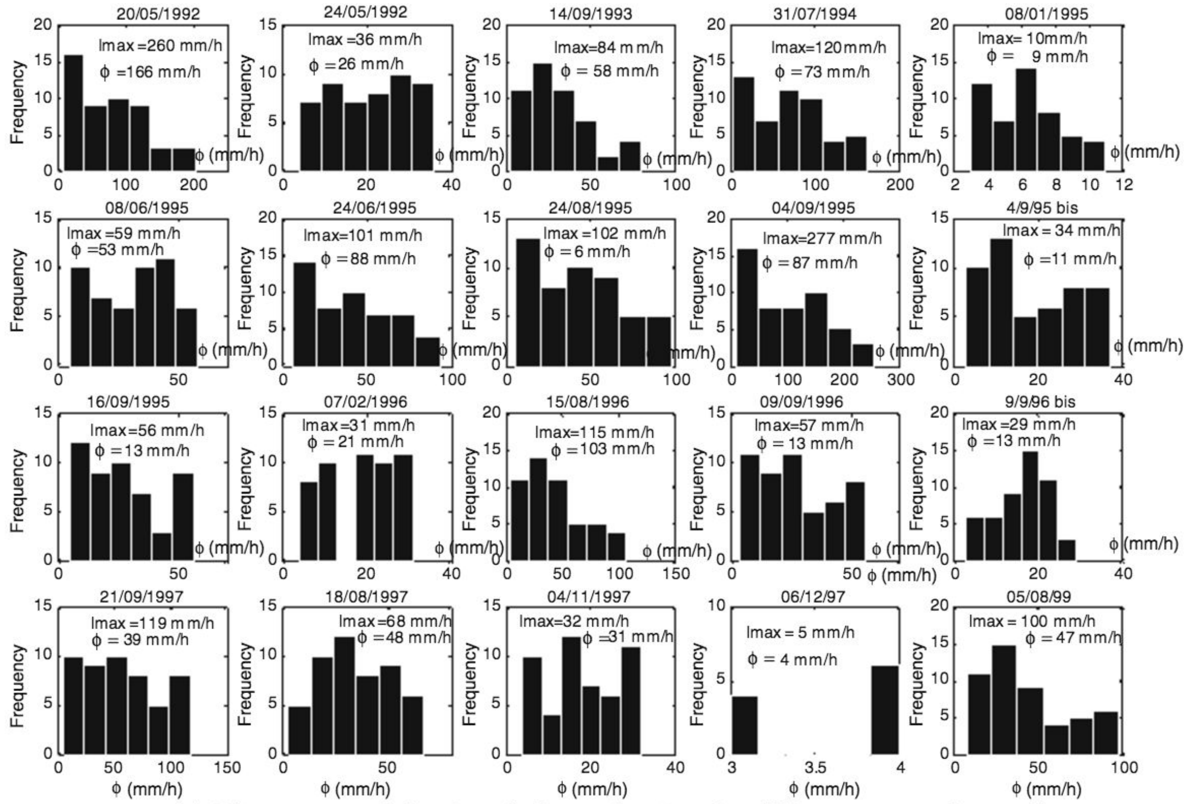

(a) Histograms of simulated ϕ knowing I_{max} for different events in mm/h

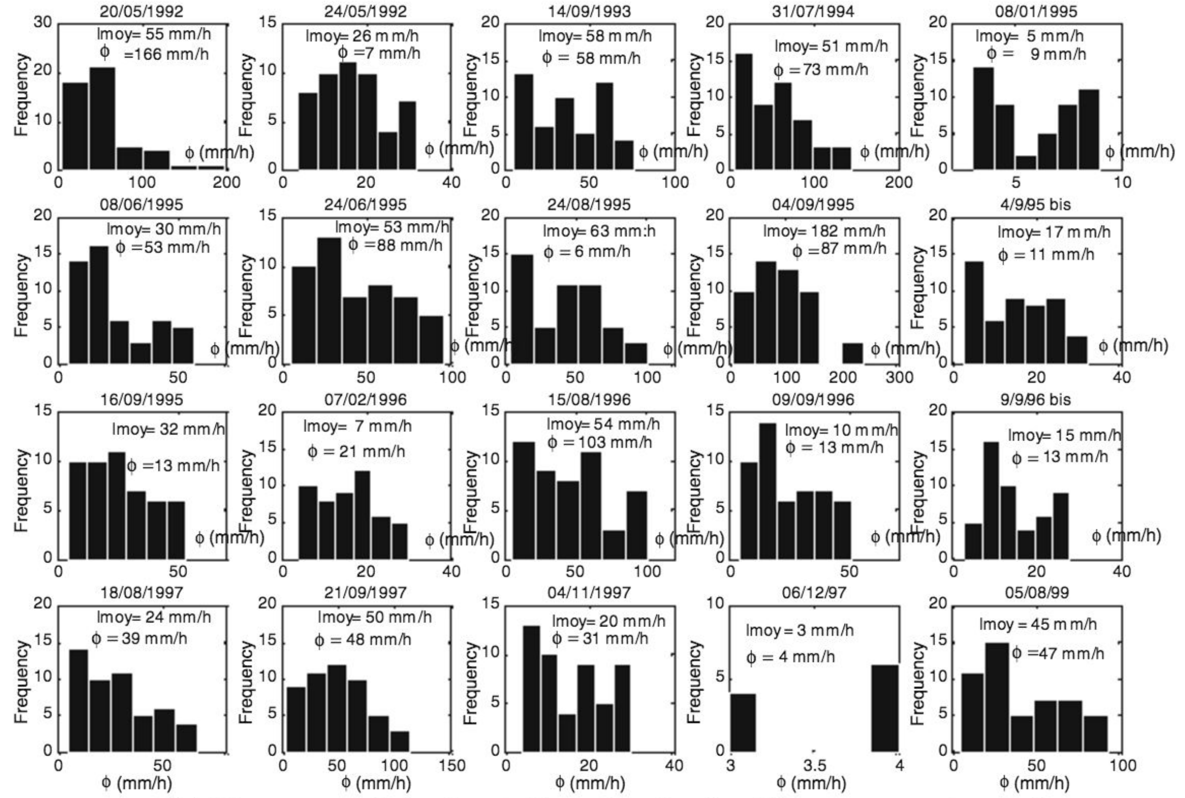

(b) Histograms of simulated ϕ knowing I_{moy} for different events in mm/h

Fig. 5 **a** Histograms of simulated ϕ knowing *Imax* for different events in mm/h. **b** Histograms of simulated ϕ knowing *Imoy* for different events in mm/h

or average) the distribution of $\phi-$index. We notice that for the high values of intensities (maximum or average) ϕ-index becomes constant.

4 Results

The methodology proposed above is simultaneously applied to effective rainfall intensities deduced from the couples (ϕ, I_{max}) and (ϕ, I_{moy}). For each event E_i, we start, using MCS by drawing ϕ conditioned to I_{max} or I_{moy}. We thus obtain a distribution$F(\phi|I_\circ)$, knowing that during the simulations of $\left(\phi|I_{moy}\right)$, ϕ is rejected if it is greater than event I_{max}. Then the vectors of effective rainfall intensities are estimated corresponding to each distribution. This procedure is repeated for the 20 selected events.

4.1 Distributions of ϕ Conditioned to I_{max} or I_{moy}

Figure 5a and b respectively represent the histograms of $(\phi|I_{\max})$ and $\left(\phi|I_{moy}\right)$ for the different analyzed events (E_i); they indicate an important dispersion of ϕ values. The latter corresponds to different states of soil moisture. Moreover, when the ratio $\phi/I_{\max}$ tends to 1, we may conclude the main part of rainfall is absorbed by the soil; and the more this ratio decreases the more the rainfall is transformed to overland flow. Contrary to the previous case, any conclusions may be drawn a priori to the rainfall transformation to overland flow for $\phi|I_{moy}$ values.

4.2 Simulated Hydrograph Analysis

The statistical interpretation of simulated hydrographs for each rainy event (E_i) is achieved with box-plots for volume (*Vi*), peak discharge (*Qpi*), peak time (*tpi*) and base time (*tbi*), thus their corresponding percentiles (25th, 50th and 75th) are analyzed. The box-plot whiskers allow analyzing the range of simulated values and the outliers. The analysis of the results is realized by the confrontation of hydrographs derived from $F_i(\phi|I_{\max})$ and$F_i\left(\phi|I_{moy}\right)$ distributions. Figure 6a to j show the box plots of the different studied characteristics.

4.2.1 Volume Analysis

Figure 6a and b show an important range of simulated volumes (*Vi*) for each event. Indeed, the mode of the variation coefficients is respectively of 0.60 and 0.87. However, for $(\phi|I_{\max})$, Fig. 6a reveals that all the observed volumes are reconstituted, and the half corresponds to a quartile; contrary to the case of $\left(\phi|I_{moy}\right)$ (Fig. 6b). In fact, the quarter of observed volumes is not reconstituted.

4.2.2 Peak Discharge Analysis

Figure 6c and d show a very important range of peak discharges (*Qpi*) with a same mode of the variation coefficients for $(\phi|I_{\max})$ and $\left(\phi|I_{moy}\right)$ equal to 0.75. In addition similarly to volumes, observed *Qpi* are integrally restituted with $(\phi|I_{\max})$ (Fig. 6c), and correspond to a quartile. On the opposite for $\left(\phi|I_{moy}\right)$ only 5 observed peak discharges, among 20 are

Fig. 6 **a** Volumes simulated from ϕ knowing *Imax* Box plots. **b** Volumes simulated from ϕ knowing *Imoy* Box plots. **c** Peak Discharge simulated from ϕ knowing *Imax* Box plots. **d** Peak Discharge simulated from ϕ knowing *Imoy* Box plots. **e** Peak time simulated from ϕ knowing *Imax* Box plots. **f** Peak time simulated from ϕ knowing *Imoy* Box plots. **g** Base time simulated from ϕ knowing *Imax* Box plots. **h** Base time simulated from ϕ knowing *Imax* Box plots ▶

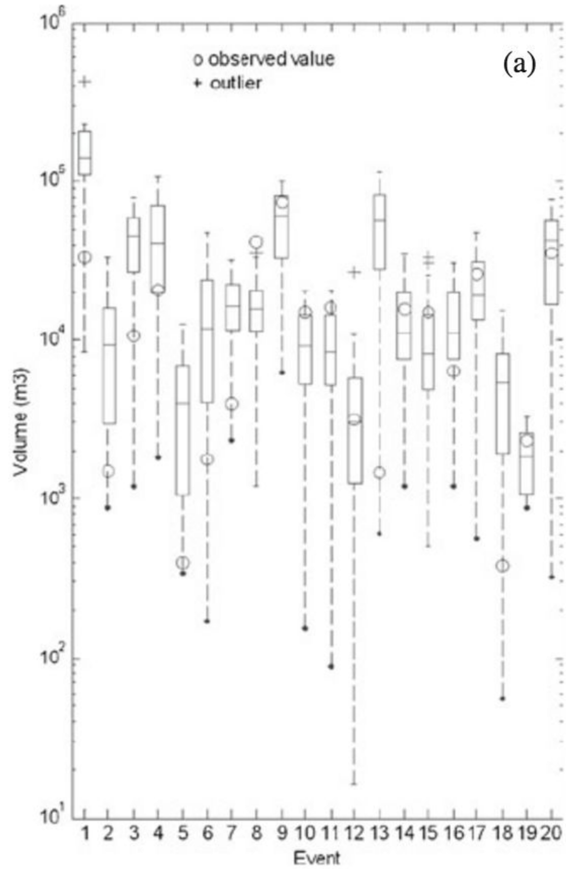

Volumes simulated from ϕ knowing I_{max} Box plots

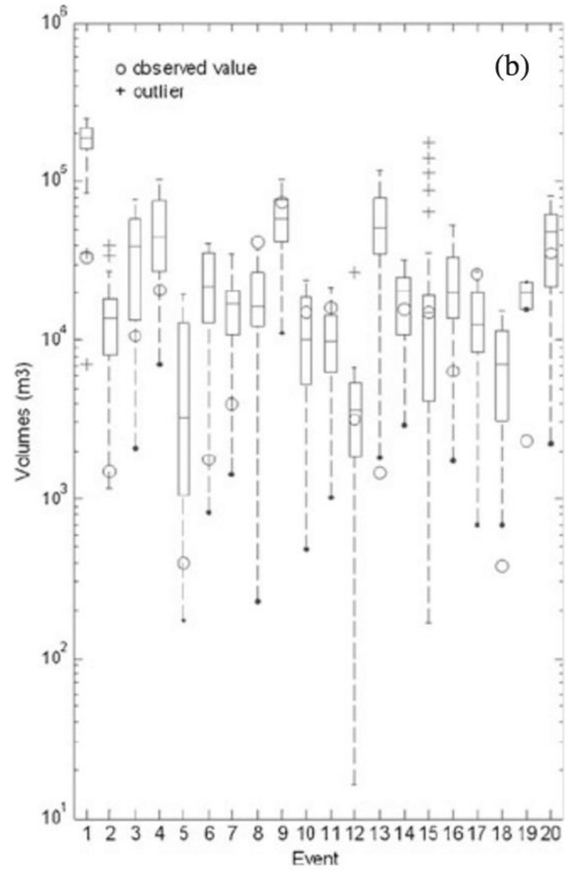

Volumes simulated from ϕ knowing I_{moy} Box plots

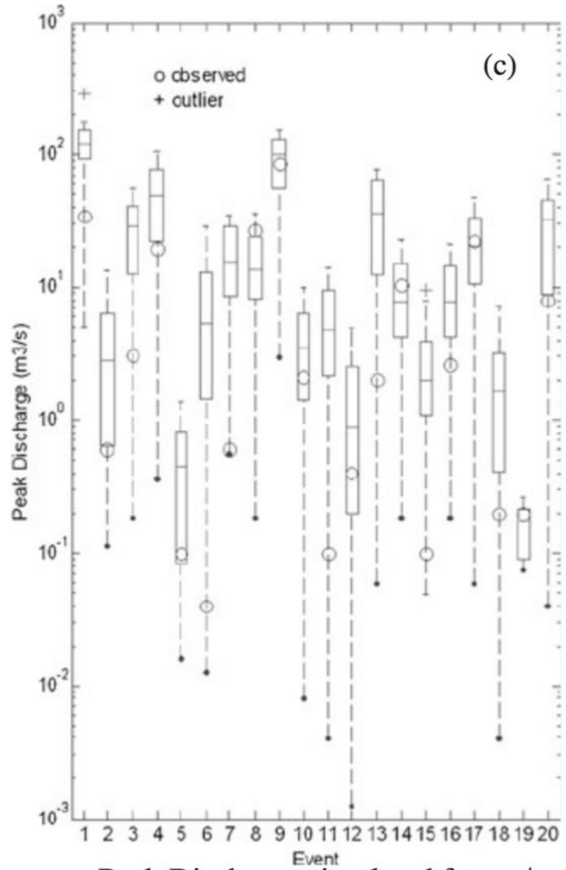

Peak Discharge simulated from ϕ knowing I_{max} Box plots

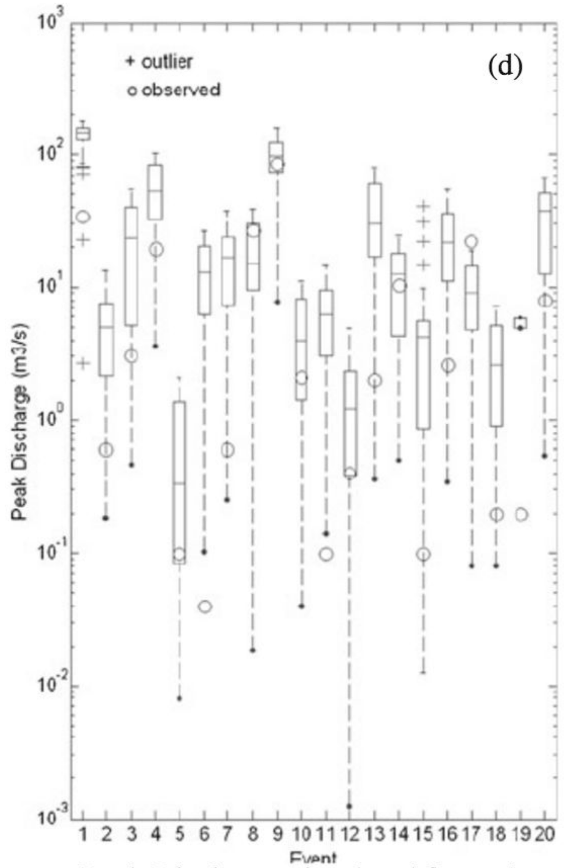

Peak Discharge simulated from ϕ knowing I_{moy} Box plots

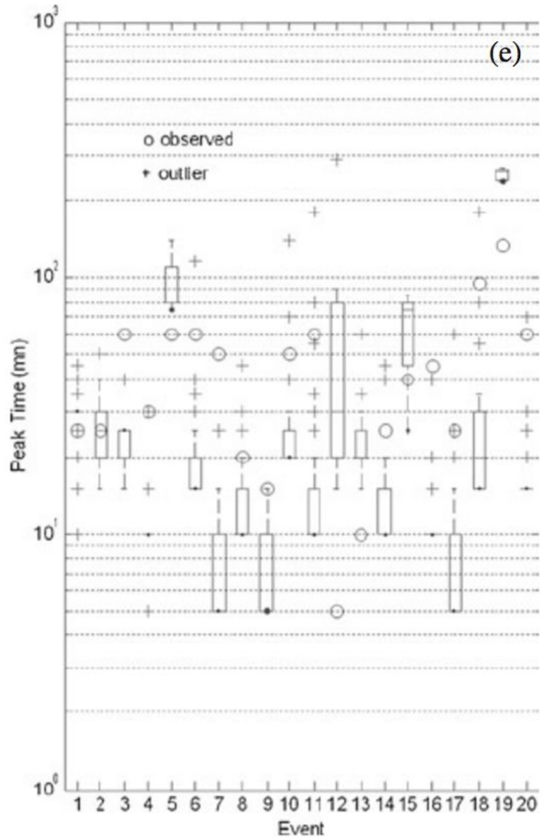

Peak time simulated from ϕ knowing I_{max} Box plots

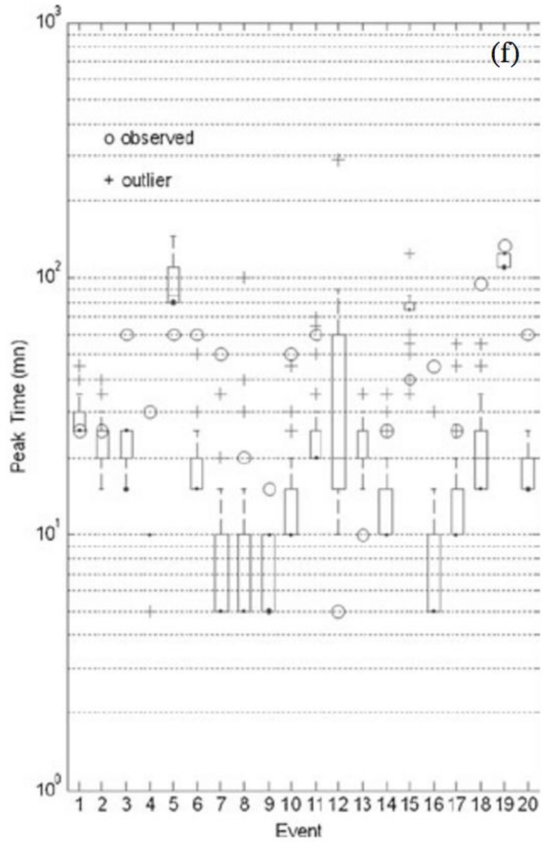

Peak time simulated from ϕ knowing I_{moy} Box plots

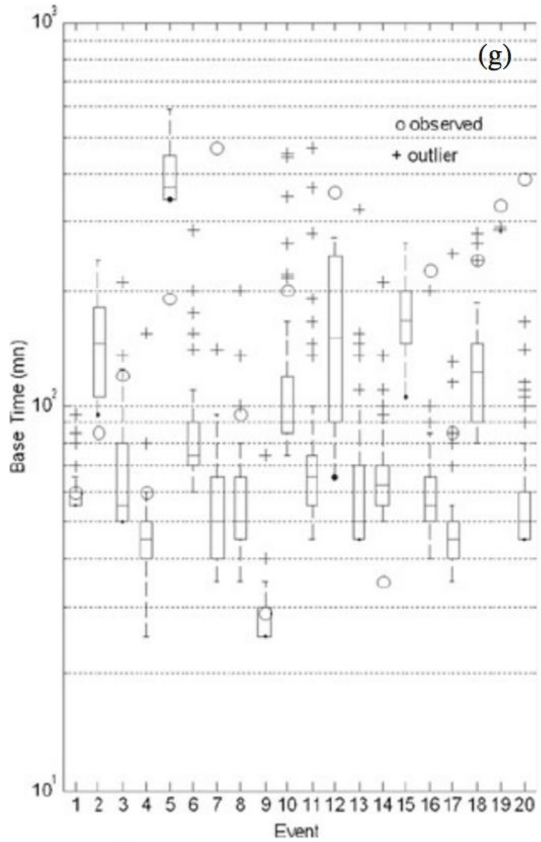

Base time simulated from ϕ knowing I_{max} Box plots

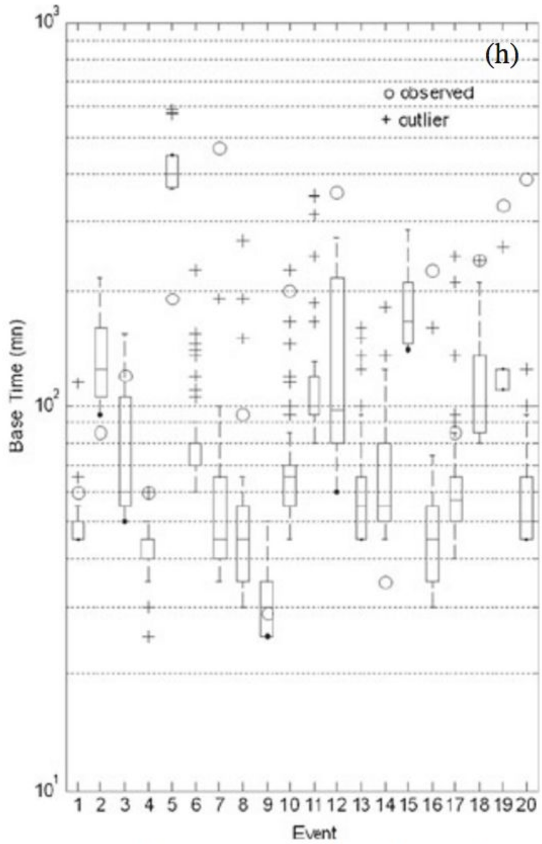

Base time simulated from ϕ knowing I_{max} Box plots

Fig. 6 (continued)

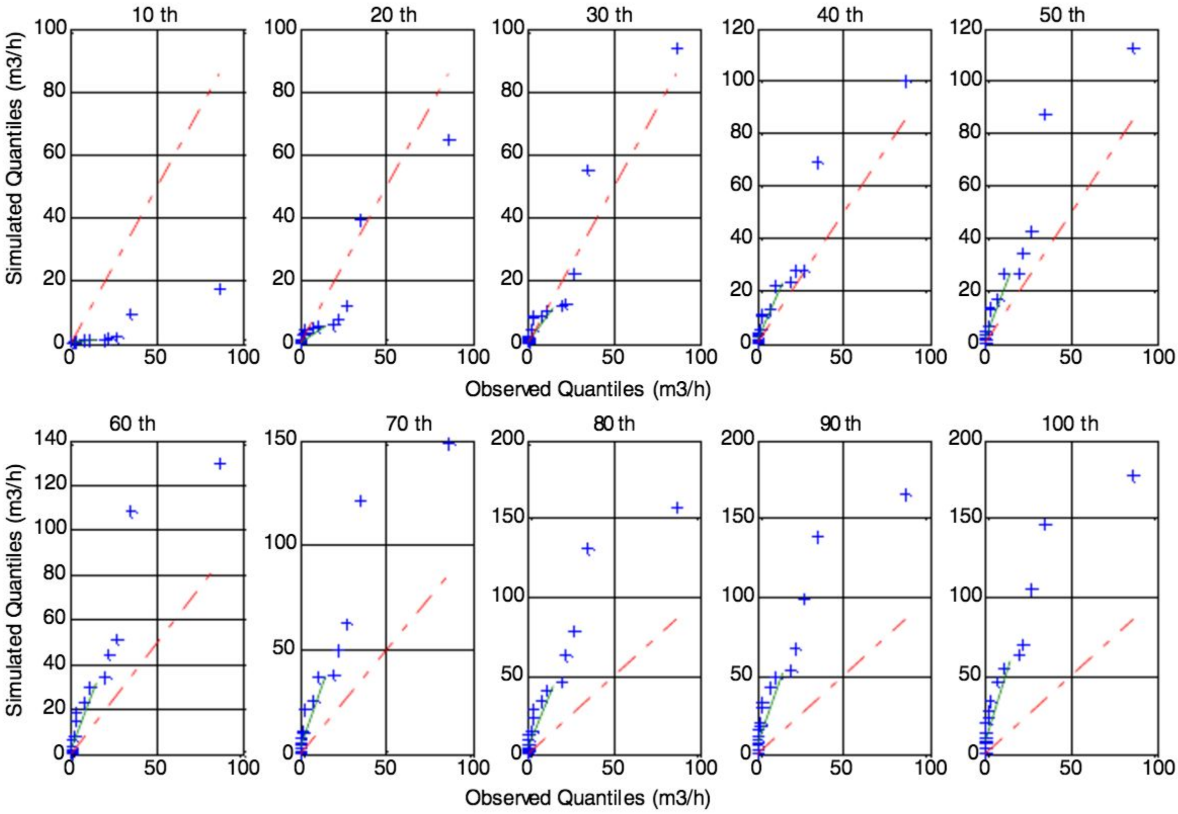

(a) Q-Q plots for simulated and observed order statistic peak discharges

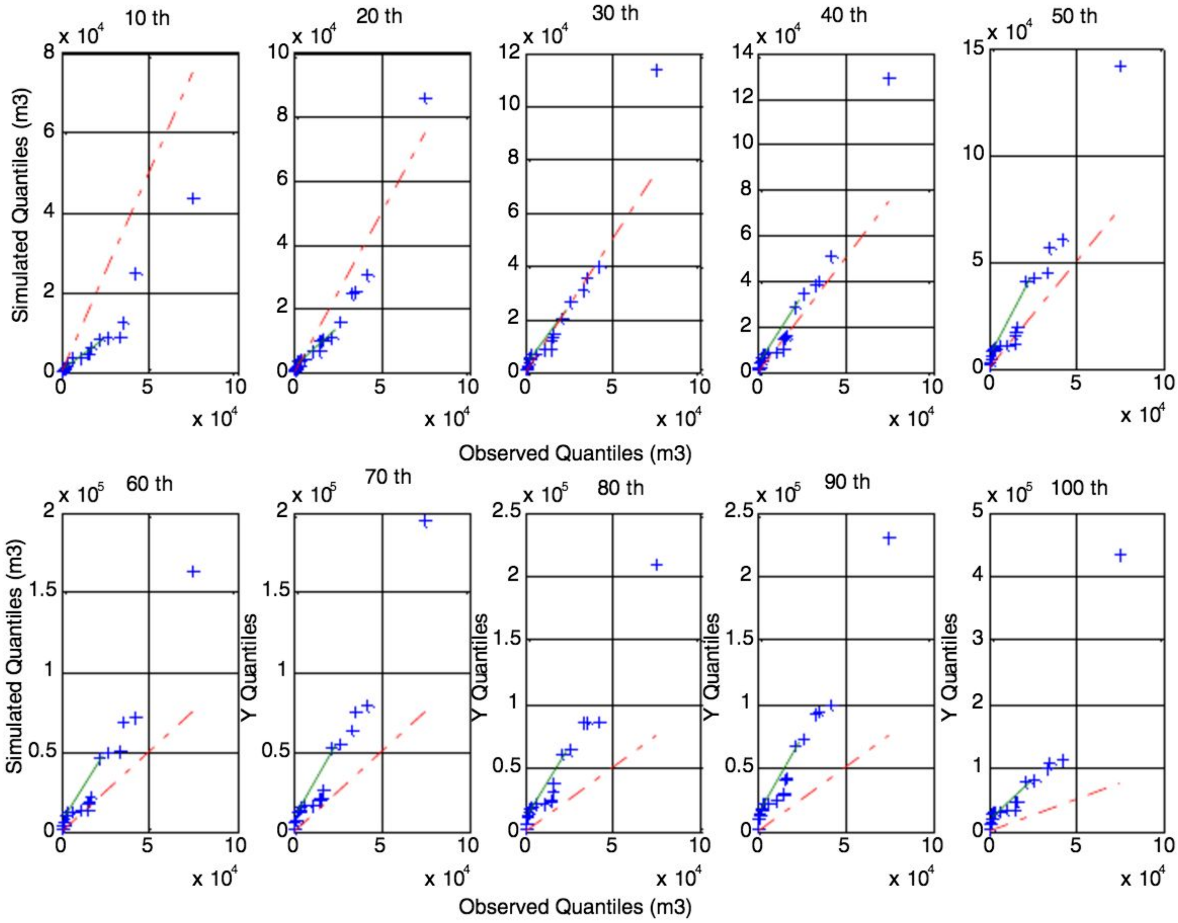

(b) Q-Q plots for simulated and observed order statistic volumes

Fig. 7 **a** Q-Q plots for simulated and observed order statistic peak discharges. **b** Q-Q plots for simulated and observed order statistic volumes restituted. It is worth noting that peak discharges which are not restituted do not necessarily correspond to restituted volumes.

4.2.3 Peak Time Analysis

The analysis of box-plots for peak time (*tpi*) (Fig. 6e and f) shows a very weak dispersion of peak time. Indeed, there are hardly whiskers on the box-plots. In addition, the mode of the variation coefficients is respectively of 0.35 and 0.41 but is not a relevant information because the time scale is of 5 min. However, we note that there are many outliers and the observed peak times are not restituted.

4.2.4 Base Time Analysis

The same conclusions may be drawn for base time (Fig. 6g and h) as above, with a mode of the variation coefficients which is respectively of 0.43 and 0.48. Most base times are not reconstituted.

5 Discussion

The obtained hydrographs from the two ϕ distributions give statistically the same results: dispersion and variability for all studied characteristics (*V*, *Qp*, *tp* et *tb*). Even if the mode of the variation coefficients for *tp* and *tb* is of 0.40 which is not relevant for the water management knowing that the time scale is of 5 min. Besides for *V* and *Qp* derived $F \times \left(\phi | I_{moy}\right)$ distribution, 40% of events are not restituted either for volume or for peak discharge or for both. Consequently the duration which is implicitly in the I_{moy} term does not improve the results, unlike what we expect. This is predictable if we examine Kendall's τ, it is more important (0.72) for the couple (ϕ, I_{max}). Thus, the hypothesis of ϕ to I_{max} conditioning is justified, and the results suggest that the formation of runoff in this catchment may be governed by rainfall kinetic energy.

6 Representative Hydrograph and Result Exploitation, Derived from (ϕ, I_{max})

In the perspective of the applicability of GIUH to ungauged basins, we propose to select the typical hydrograph which represents the catchment behavior, by constituting the series of order statistics corresponding to each output, and using Q-Q plots to compare each order statistics set to the observed one. In this work, the main interest outputs are the peak discharge or the volume. In accordance with the interest output, the order statistics set which proves the best by comparison to the observed hydrograph component (volume or peak discharge) is the representative hydrograph or design hydrograph.

Figure 7a and b show Q-Q plots for *Qp* and *V*. We notice that for the order statistics corresponding to 30th percentile of *Qp* as well that of *V*, the same conclusion can be drawn. The simulated sets come from populations with common distribution as the observations. Indeed, the points fall near the 45 reference line. Consequently, we assume that the hydrograph of the order statistic corresponding to 30th percentile of the volumes or the peak discharges represents the typical hydrograph of the catchment behavior, for fixed I_{max}.

We therefore can propose a methodology for the determination of the design hydrograph which is illustrated by Fig. 8.

7 Conclusions

In order to apply the GIUH to ungauged basins, MCS are achieved for generating hydrographs. The dispersion of their characteristics (volume, peak discharge, peak time and base time) is analyzed, and allowed selecting the design hydrograph. The effective rainfall input of GIUH model is considered here as unknown and is estimated with infiltration index method (ϕ-index). Three main correlations are detected and tested between this index and the characteristic rainfall intensities: maximum intensity average intensity and duration. They are modeled with Archimedean copulas. Consequently, assuming $F(\phi|X)$ distributions, the effective rainfall hyetographs are generated. It appears that:

- The conditioning of ϕ-index to D disables the reconstitution of the observed values. At this step of this research, no conclusions can be drawn. Other types of copulas which model negative correlations have to be tested.
- The resulting hydrographs from the two ϕ distributions give statistically the same results: dispersion and variability for all studied characteristics (*V*, *Qp*, *tp* et *tb*).
- The effective rainfall hyetographs derived from $F(\phi|I_{\max})$ distribution allowed reconstituting the observed hydrographs; unlike the case of $F(\phi|I_{moy})$ which deals with rainfall duration (I_{moy} is the ratio between rainfall depth and duration). The average intensity does not seem to improve the results.
- The encouraging results derived from $F(\phi|I_{\max})$ distribution allow supporting the hypothesis of the conditioning of ϕ to I_{max}. Moreover, they suggest that the kinetic rainfall energy may control the runoff.
- Other investigations may be possible between ϕ and other variables such as the antecedent rainfall or kinetic rainfall energy.
- The comparison between the series of order statistics corresponding to interest output and those corresponding to the observed series of order statistics leads to select the design catchment hydrograph.

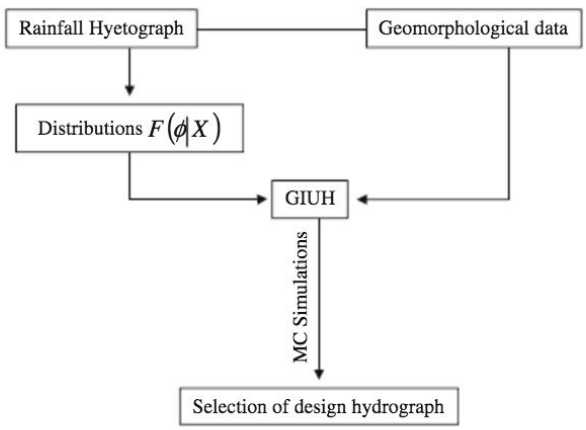

Fig. 8 Methodological diagram for design hydrograph for ungauged basins

Appendix 1

Table 5 Several references published copula models. One famous reference: Nelsen (1999) who presented among these models, the Archimedean ones and particularly those of one parameter. The following table shows the copula generators and the relation between the copula parameter and Kendall's τ

One parameter Archimedean copulas	Generator	Relation between copula parameter a and Kendall's τ
Frank	$\varphi(t) = -\ln\left(\frac{e^{-at}-1}{e^{-a}-1}\right)\ a \neq 0$	$\tau(a) = 1 - \frac{4}{a} + \frac{4}{a^2}\int_0^a \frac{t}{e^t-1}dt$
Gumbel	$\varphi(t) = (-\ln(t))^a\ a > 0$	$\tau(a) = 1 - 1/a$
Clayton	$\varphi(t) = a\left(t^{-1/a} - 1\right)\ \ a > 0$	$\tau(a) = 1/(2\,a + 1)$

Appendix 2

***K(z)* function:** is the distribution function of the copula *C(U,V)*. Genest and Rivest (1993) showed that this distribution function is related to the generator φ of an Archimedean copula through the expression of *K*(*z*):

$$K(z) = z - \varphi(z)/\varphi'(z) \tag{A2.1}$$

An empirical *K(z)* can be calculated for any *z* as the proportion of empirical values of *C(u, v)* that is less than *z*:

$$K_{\text{emp}}(z) = \{\text{number } of\ z_i \leq\ z\}/n \tag{A2.2}$$

***J(z)* function or cumulative τ :** tau is related to a copula through the expression:

$$\tau = -1 + 4\int_0^1\int_0^1 C(u,v)c(u,v)\mathrm{d}u\mathrm{d}v \tag{A2.3}$$

J(z) function is expressed by:

$$J(z) = -1 + 4\left(\int_0^z\int_0^z C(u,v)c(u,v)\mathrm{dudv}\right)/C(z,z)^2 \tag{A2.4}$$

The full double integral is a probability weighted average of *C(u,v)*. To compare this, the partial integral has to be divided by the weights, thus the first power of C(*z, z*) is the denominator. This quotient gives the average value of *C(u,v),* which increases as a function of *z*. The second *C(z, z)* divisor expresses this average relative to *C*(*z, z*). It should be that $J(1) = \tau$.

An empirical cumulative tau can also be calculated, expressed by:

$$J(z) = -1 + 4I(z)/C(z,z)^2 \tag{A2.5}$$

Where *I*(*z*) is defined by $I(z) = \frac{1}{n}\sum_{i=1}^{n} z_i \times \mathrm{I}\{u_i < z\, et\, v_i\ < z\}$, with **I** is the indicator function.

***M*(*z*) function** is the cumulative conditional mean defined by:

$$M(z) = E(V|U < z) = \left(\int_{u=0}^{z} \int_{v=0}^{1} v \cdot c(u,v) \mathrm{d}u \mathrm{d}v \right) / z \tag{A2.6}$$

Verifying *M*(1)=1/2.

Let *D*(*z*) $D(z) = \sum_{i=1}^{n} \mathrm{I}\{u_i < z\}$ and $N(z) = \sum_{i=1}^{n} v_i \mathrm{I}\{u_i < z\}$, the empirical version of *M*(*z*) is expressed by:

$$M(z) = N(z)/D(z) \tag{A2.7}$$

With *D*(1)=*n* and *N*(1)=*n*/2.

***L*(*z*) and *R*(*z*) functions** are *Left* and *Right* tail concentration functions. The two functions *L*(*z*) and *R*(*z*) are:

$$L(z) = P(U < z, V < z)/z = C(z,z)/z \tag{A2.8}$$

$$R(z) = P(U > z\ ,\ V > z)/(1-z) = (1 - 2z + C(z,z))/(1-z) \tag{A2.9}$$

Joe (1997) defined lower tail dependence parameter for *L(0)* = $\lambda_{\min} = \lim_{u \to 1} P(Y \le F_Y^{-1} \times (u) \big| X \le F_X^{-1}(u)) = \lim_{z \to 0} L(z)$ (left tail), and upper tail dependence parameter for *R (1)* = $\lambda_{\max} = \lim_{u \to 1} P(Y > F_Y^{-1}(u) \big| X > F_X^{-1}(u)) = \lim_{z - 1} R(z)$ (right tail).

L function is analyzed for $z \in \left[0, \frac{1}{2}\right]$ and *R* function for all $z \in \left[\frac{1}{2}, 1\right]$.

Appendix 3

Let (*X,Y*) be a sample of size *n*.

The X_i and Y_i are regrouped into 6 classes respectively $(v_0; v_1]$; $(v_1; v_2]$; …; $(v_5; v_6]$, and $(w_0; w_1]$; $(w_1; w_2]$; …; $(w_5; w_6]$, where the boundaries v_i's (w_i) are chosen such that the number of observations $\lambda_1, \lambda_2 \ldots, \lambda_6$ respectively $\eta_1, \eta_2 \ldots, \eta_6$, in the corresponding classes are as symmetrically distributed as possible. We thus obtain 36 two-dimensional intervals $(v_{i-1}; v_i]$ x $(w_{i-1}; v_i]$, *i,j*=*1….6*. Then we regroup these intervals in *k* larger rectangular interval classes, such that an expected frequency of at least 1% in each class and a 5% expected frequency in 80% of the classes. The fitted number of observations $f_{i,j}$ in each 36 two-dimensional intervals $(v_{i-1}; v_i]$ x $(w_{i-1}; v_i]$, is given by:

$$f_{i,j} = n\left[\left(F(v_i), F(w_j)\right) - \left(F(v_{i-1}), F(w_j)\right) - \left(F(v_i), F(w_{j-1})\right) + \left(F(v_{i-1}), F(w_{j-1})\right)\right]$$
$$i,j = 1.....6, \quad F(x,y) = C(F_X(x), F_Y(y)) \tag{A3.1}$$

Let $z_{i,j}$ be the number of observations in the 36 two-dimensional intervals. Through summation of $z_{i\ j}$'s respectively $f_{i;j}$'s, one obtains the number of observations O_k, respectively, the expected number of observations E_k, in each rectangular interval class *k*. The bivariate Chi-square statistic is then defined by:

$$\chi^2 = \sum_{k=1}^{m} (O_k - E_k)^2 / E_k \tag{A3.2}$$

References

Bárdossy A (2006) Copula-based geostatistical models for groundwater quality parameters. Water Resour Res 42:W11416. doi:10.1029/2005WR004754

Bárdossy A, Li J (2008) Geostatistical interpolation using copulas. Water Resour Res 44:W07412. doi:10.1029/2007WR006115

Bárdossy A, Mascellani G, Franchini M (2006) Fuzzy unit hydrograph. Water Resour Res 42:W02401. doi:10.1029/2004WR003751

Beven KJ (2003) *Rainfall-runoff modeling*: *the primer*. Wiley, England, p 372

Bhadra A, Panigrahy N, Singh R, Raghuwanshi NS, Mal BC, Tripathi MP (2008) Development of a geomorphological instantaneous unit hydrograph model for scantily gauged watersheds. Environ Model Software 23:1013–1025

Bhunya PK, Berndtsson R, Ojha CSP, Mishra SK (2007) Suitability of Gamma, Chi-square, Weibull, and Beta distributions as synthetic unit hydrographs. J Hydrol 334:28–38

Bhunya PK, Berndtsson R, Singh PK, Hubert P (2008) Comparison between Weibull and gamma distributions to derive synthetic unit hydrograph using Horton ratios. Water Resour Res 44:W04421. doi:10.1029/2007WR006031

Chandramohan T, Venkatesh B, Jain SK (2002) Rainfall-runoff modelling based on GIUH approach in a GIS environment. J Instn Eng 83:180–185

Cudennec C (2007) DISCUSSION of "Coding random self-similar river networks and calculating geometric distances: 1. General methodology" and "2. Application to runoff simulations" on width function-based unit hydrographs deduced from separately random self-similar river networks and rainfall variability. Hydrol Sci J 52(1):230–237

Cudennec C, Fouad Y, Sumarjo GI, Duchesne J (2004) A geomorphological explanation of the unit hydrograph concept. Hydrolog Process 18(4):603–621. doi:10.1002/hyp. 1368

De Michele C, Salvadori G (2003) A generalized pareto intensity–duration model of storm rainfall exploiting 2-copulas. J Geophys Res 108(D2):15-1–15-2

De Michele C, Salvadori G, Canossi M, Petaccia A, Rosso R (2005) Bivariate statistical approach to spillway design flood. J Hydrol Eng ASCE 10(1):50–57

Eagleson PS (1970) Dynamics hydrology. EGU Reprint Series, 2, 2003, 37191 Katlenburg-Lindau, Germany.

Eagleson PS (1972) Dynamics Flood Frequency. Water Resour Res 8(4):878–898

Ellouze-Gargouri E, Kebaili-Bargaoui Z (2006) Prédétermination des débits maximaux de crue par simulation Monte-Carlo de la pluie nette. Rev Sci Eau 19(4):327–345

Favre AC, El Adlouni S, Perreault TL, Thiemonge N, Bobée B (2004) Multivariate hydrological frequency analysis using copulas. Water Resour Res 40(W01101):1–12

Fleurant C, Kartiwa B, Roland B (2006) Analytical model for a geomorphological instantaneous unit hydrograph. Hydrol Process 20(18):3879–3895

Franchini M, O'Connell PE (1996) An analysis of the dynamic component of the geomorphologic instantaneous unit hydrograph. J Hydrol 175:407–428

Gargouri-Ellouze E, Bargaoui Z (2009) Investigation with Kendall plots of infiltration index–maximum rainfall intensity relationship for regionalization. J Phys Chem Earth. doi:10.1016/j.pce.2009.02

Gargouri-Ellouze E, Chebchoub A (2008) Depth—duration—frequency with copulas. Hydrol Sci J 53(4):802–817

Genest C, Favre AC (2007) Everything you always wanted to know about copula modeling but were afraid to ask. J Hydrol Engng ASCE 12:347–368

Genest C, Mackay RJ (1986) Copules archimédiennes et familles de lois bidimensionnelles dont les marges sont données. Rev Can Statis 14:145–159

Genest C, Rivest L (1993) Statistical inference procedures for bivariate Archimedean copulas. J Am Statis Assoc 88:1034–1043

Goel NK, Kurothe RS, Mathur BS, Vogel RM (2000) A derived flood frequency distribution of correlated rainfall intensity and duration. J Hydrol 228:56–67

Grimaldi S, Serinaldi F, Napolitano F, Ubertini L (2005) A 3-copula function application for design hyetograph analysis. In: Savic DA, Mariño MA, Savenije HHG, Bertoni JC (eds) Sustainable water management solutions for large cities. IAHS, Wallingford, pp 293–212

Gupta VK, Mesa OJ (1988) Runoff generation and hydrologic response via channel network geomorphology —recent progress and open problems. J Hydrol 102:3–28

Gupta VK, Waymire E (1983) On the formulation of an analytical approach to hydrologic response and similarity at the basin scale. J Hydrol 65:95–123

Gupta VK, Waymire E, Wang CT (1980) A representation of an instantaneous unit hydrograph from geomorphology. Water Resour Res 16(5):855–862

Hermassi T (2000) Analyse des facteurs conditionnels de l'écoulement et de l'érosion dans de petits bassins verssants de la Dorsale tunisienne, M.S. thesis, 68 pp., Institut National Agronomique de Tunisie
Horton RE (1933) The role of infiltration in hydrologic cycle. Trans Am Geophys Union 14:446–460
Hürlimann W (2004) Fitting bivariate cumulative returns with copulas. Comp Statis Data Anal 45:355–372
Jain V, Sinha R (2003) Derivation of unit hydrograph from GIUH analysis for a Himalayan river. Water Resour. Management 17(5), 355–376(22)
Jain SK, Singh RD, Seth SM (2000) Design flood estimation using GIS supported GIUH approach. Water Resour Manag 14(5):369–376
Jin C-X (1992) A deterministic gamma-type geomorphologic instantaneous unit hydrograph based on path types. Water Resour Res 28(2):479–486
Joe H (1997)Multivariate models and dependence concepts. In: Monographs on Statistics and applied probability. Chapman and Hall, London
Karlinger MR, Troutman BM (1985) Assessment of the instantaneous unit hydrograph derived from the theory of topologically random networks. Water Resour Res 21(11):1693–1702
Kumar R, Chatterjee C, Lohani AK, Kumar S, Singh RD (2002) Sensitivity Analysis of the GIUH based Clark Model for a Catchment. Water Resour. Management 16 (4), 263–278(16)
Kumar R, Chatterjee C, Singh RD, Lohani AK, Kumar S (2004) GIUH based Clark and Nash models for runoff estimation for an ungauged basin and their uncertainty analysis. Intl J River Basin Manag 2 (4):281–290
Kumar R, Chatterjee C, Singh RD, Lohani AK, Kumar S (2007) Runoff estimation for an ungauged catchment using geomorphological instantaneous unit hydrograph (GIUH) models. Hydrol Process 21(14):1829–1840
Kurothe RS, Goel NK, Mathur BS (1997) Derived flood frequency distribution for negatively correlated rainfall intensity and duration. Water Resour Res 33(9):2103–2107
Kurothe RS, Goel NK, Mathur BS (2001) Derivation of a curve number and kinematic-wave based flood frequency distribution. Hydrol Sci J 46(4):571–583
Moussa R (2008) Effect of channel network topology, basin segmentation and rainfall spatial distribution on the geomorphologic instantaneous unit hydrograph transfer function. Hydrol Process 22:395–419
Musy A, Higy C (2004) Hydrologie générale, une science de la nature. Presse Polytechnique Universitaire Romande, Lausanne, p 314
Nadarajah S (2007) Probability models for unit hydrograph derivation. J Hydrol 344:185–189
Nash JE (1959) Systematic determination of unit hydrograph parameters. J Geophys Res 64(1):111–115
Nasri S, Cudennec C, Albergel J, Berndtsson R (2004) Use of a geomorphological transfer function to model design floods in small hillside catchments in semiarid Tunisia. J Hydrol 287:197–213
Nelsen RB (1999) An Introduction to Copulas. Springer, New York
Nowicka B, Soczynska U (1989) Application of GIUH and dimensionless hydrograph models in ungauged basins. In: *FRIENDS in Hydrology* (ed. by L. Roald, K. Nordseth and K.A. Hassel), Proc. Bolkesjø Symp., Inter. Assoc. Hydrol Sci Pubn 187, 197–203
Prokhorov AV (2002) Kendall coefficient of rank correlation. In: Michiel H (ed) Encyclopaedia of mathematics. CWI, Amsterdam
Rodriguez-Iturbe I, Valdès JB (1979) The geomorphologic structure of hydrologic response. Water Resour Res 15:1409–1420
Rodriguez-Iturbe I, Gonzalez-Sanabria M, Brass RL (1982) A geomorphoclimatic theory of instantaneous unit hydrograph. Water Resour Res 18(4):877–886
Rosso R (1984) Nash model relation to Horton order ratios. Water Resour Res 20(7):914–920
Sahoo B, Chatterjee C, Raghuwanshi NS, Singh R, Kumar R (2006) Flood estimation by GIUH-Based Clark and Nash models. J Hydrol Eng 11(6):515–525
Salvadori G, De Michele C (2006) Statistical characterization of temporal structure of storms. Adv Water Resour 6:827–842
Sarangi A, Madramootoo C, Enright P, Prasher S (2007) Evaluation of three unit hydrograph models to predict the surface runoff from a Canadian watershed. Water Resour Management 21 (7) 1127–1143 (17).
Schweizer B, Sklar A (1983) Probabilistic metric spaces. Elsevier, Amsterdam
Soil Conservation Service (SCS) (1957) Use of storm and watershed characteristics in synthetic hydrograph analysis and application. US Department of Agriculture, Soil Conservation Service, Washington
Troutman BM, Karlinger MR (1985) Unit hydrograph approximations assuming linear flow through topologically random channel networks. Water Resour Res 21(5):743–754
Valdès JB, Fiallo Y, Rodriguez-Iturbe I (1979) A rainfall-runoff analysis of the geomorphologic IUH. Water Resour Res 15(6):1409–14520

van der Tak LD, Brass RL (1990) Incorcorating hillslope effects into the geomorphologic instantaneaous unit hydrograph. Water Resour Res 26(10):2393–2400

Venter G (2002) Tails of copulas. Proc Casualty Actuarial Society 89:68–113

Venter G (2003) Quantifying correlated reinsurance exposures with copulas. Casualty Actuarial Society Forum 2003:215–229

Zhang L, Singh VP (2006) Bivariate flood frequency analysis using the copula method. J Hydrol Eng 11 (2):150–164